

GENERALIZED LINEAR TARGETING FOR CISLUNAR FLIGHT

David Geller*, **Brayden Barton** [†], **David Woffinden** [‡]

An important element of Artemis and NASA's campaign to explore the Moon is the autonomous onboard two-level targeter (TLT) used during all cislunar flight phases. The function of the TLT is to autonomously recompute the burn targets for the upcoming burn (or multiple burns) in response to navigation and vehicle dispersion providing a solution that meets all of the trajectory constraints. Although the TLT has been utilized previously as a ground-based planning tool, and flown onboard during the Artemis I mission, its complexity and iterative nature make it difficult to incorporate into and support rapid analyses such as robust optimal trajectory design applications where speed is essential. In this paper, a set of generalized linear targeting algorithms that mimics many of the properties of the TLT is derived. The generalized algorithms can handle single or multiple impulsive maneuvers, with multiple constraints at multiple fixed or variable times. A linear targeting algorithm for finite burn maneuvers is also derived. The generalized linear targeting algorithms are exceptionally fast and easy to implement in Monte Carlo analysis, linear covariance (LinCov) analysis, and robust optimal trajectory design. Several cislunar flight examples are provided.

INTRODUCTION

The Orion autonomous onboard two-level targeter (TLT) was successfully utilized during the Artemis I mission for all phases of cislunar flight.¹ The function of the TLT is to autonomously recompute the burn targets for the upcoming burn (or multiple burns) in response to navigation and vehicle dispersion, subject to trajectory constraints. The algorithm consists of two main processes:^{1,2,3,4} the Level 1 process runs sequentially through the patch states, propagating each state to the time of the next patch point and iteratively applying either an instantaneous Δv or a burn arc to enforce position continuity along the trajectory. After the Level 1 process is complete, the Level 2 process simultaneously adjusts the positions and times of each patch state to meet any applied trajectory constraints. Because the Level 2 process typically has more control parameters than constraints, a minimum norm solution is used to compute the desired updates. After the Level 2 updates are applied, the algorithm goes back through the Level 1 process, and continues to cycle iteratively through the Level 1 and Level 2 until it achieves a trajectory that is continuous in position and meets all of the applied trajectory constraints.

Although the TLT was successfully used in flight during the Artemis I mission, its complexity and iterative nature make it difficult to use for rapid analysis where speed is essential. This is particularly applicable when robust trajectory design techniques are utilized. Non-linear targeting algorithms for

*Distinguished Scientist/Engineer, Strategy Military Space Division, Utah State University Space Dynamics Laboratory, 1695 North, Research Park Pkwy, North Logan, UT, 84341

[†]Graduate Student, Mechanical and Aerospace Engineering Department, Utah State University, 4130 Old Main Hill, Logan, UT, 84321

[‡]Aerospace Engineer, GN&C Autonomous Flight Systems Branch, NASA Johnson Space Center, Houston TX, 77058

cis-lunar applications such as the TLT have proven to be too slow when a large number of runs in a Monte Carlo or linear covariance environment are required. For Monte Carlo analysis the issue is primarily the time it takes to execute the TLT prior to each maneuver. For LinCov analysis this issue is exacerbated since LinCov requires the partial derivative of the maneuver with respect to the vehicle position and velocity, and this entails calling the TLT six times for each maneuver to compute the required numerical partial derivatives.

To overcome these issues, this paper derives a set of generalized targeting algorithm based on a linearization of the problem. The resulting linear targeting algorithms mimic many of the TLT properties and features, and while they may not be appropriate for flight, their exceptionally fast execution and easy to derive partial derivatives make them extremely useful for Monte Carlo analysis, LinCov analysis, and robust optimal trajectory design. It is important to note that although the TLT is a nonlinear targeting algorithm, its underlying elements are based on a linearization of the problem, and during the Artemis I mission the TLT required no more than 3 iterations to converge.¹ This lends credibility to the generalized linear algorithms derived in this paper.

In the next section, three linear impulsive maneuver targeting algorithms will be derived. The first targeting algorithm is for a single impulsive maneuver subject to an arbitrary number of constraints at a single fixed or variable final time. The second targeting algorithm is for a single impulsive maneuver subject to an arbitrary number of constraints at multiple fixed or variable times, and the third linear targeting algorithm is for multiple impulsive maneuvers subject to an arbitrary number of constraints at multiple fixed or variable times. Several cislunar targeting examples will be provided.

The theory is then extended to include a linearized finite-burn targeting algorithm subject to an arbitrary number of constraints at a single fixed or variable final time. The controls to be solved for are the engine ignition time, direction and rotation rate of the thrust vector, the thrust cutoff time, and an optional variable final time. An example of finite-burn targeting for powered lunar ascent will be presented. This will be followed by final comments and conclusions.

THE WELL-DEFINED, OVER-DETERMINED, AND UNDER-DETERMINED PROBLEMS

All of the derivations below result in a set of m linear equations of the following form

$$\mathcal{M}\delta u = \mathcal{N}\delta x_0 \quad (1)$$

where δu represents n controls to be solved for, and δx_0 represents the initial position and velocity dispersion from the nominal reference trajectory. For finite burns, δx_0 may also include the initial mass dispersion and initial thrust I_{sp} dispersion.

For the impulsive targeting algorithms the n controls are single or multiple impulsive Δv maneuvers and variable constraint times. For the finite-burn targeting algorithm, the n controls are the engine ignition time, direction and rotation rate of the thrust vector, the thrust cutoff time, and an optional variable constraint time. When $m = n$, Eq. 1 represents a well-defined problem whose solution is simply

$$\delta u = \mathcal{M}^{-1}\mathcal{N}\delta x_0 \quad (2)$$

When $m > n$, Eq. 1 represents an over-determined problem and a solution for the minimum constraint error norm is desired

$$\delta u = (\mathcal{M}^T W_\psi \mathcal{M})^{-1} \mathcal{M}^T W_\psi \mathcal{N}\delta x_0 \quad (3)$$

where the constraints are weighted by a diagonal matrix W_ψ . When $m < n$, Eq. 1 represents an under-determined problem and a solution to the minimum control norm is desired [Define W_c]

$$\delta u = W_c \mathcal{M}^T (\mathcal{M} W_c \mathcal{M}^T)^{-1} \mathcal{N} \delta x_0 \quad (4)$$

Depending on how the targeting algorithms derived below are formulated, i.e., $m = n$, $m > n$, or $m < n$, one of the above three solutions to Eq. 1 will be available.

DERIVATION OF A LINEAR IMPULSIVE MANEUVER TARGETING ALGORITHM

When position and velocity dispersion from a desired nominal trajectory are zero, all trajectory constraints will by definition be satisfied. However, when position and velocity dispersion are non-zero, a single or multiple corrective impulsive maneuvers may be required to meet mission constraints. The objective of this section is to derive three impulsive maneuver targeting algorithms, each more general than the previous, to correct for initial trajectory dispersion and ensure trajectory constraints are satisfied.

Single Maneuver Δv With Arbitrary Number of Constraints at a Single Fixed or Variable Final Time

This targeting algorithm is a generalization of what is commonly called Clohessy-Wiltshire (CW) targeting, or, in the fixed-final time case, a generalized and linearized version of Lambert targeting.

Let $\psi_f(x_f) = 0$ represent m nonlinear constraints that must be satisfied by the final inertial position and velocity state vector x_f , at a variable final time $t_f^* + \delta t_f$, where δt_f is a control parameter that needs to be determined. The nominal final state vector x_f^* must also satisfy the constraints at the nominal final time t_f^* , i.e., $\psi_f(x_f^*) = 0$. If the non-contemporaneous⁵ final state x_f is given by $x_f = x_f^* + \delta x_f + \dot{x}_f^* \delta t_f$, the m nonlinear constraints can be linearized about the nominal position and velocity state vector x_f^*

$$\psi_f(x_f) = \psi_f(x_f^*) + \frac{\partial \psi_f}{\partial x_f} \Big|_{x_f^*} (\delta x_f + \dot{x}_f^* \delta t_f) \quad (5)$$

This reduces to

$$\Psi_{x,f}(\delta x_f + \dot{x}_f^* \delta t_f) = 0, \quad \text{where } \Psi_{x,f} = \frac{\partial \psi_f}{\partial x_f} \Big|_{x_f^*} \quad (6)$$

Using linearized discrete-time dynamics, the contemporaneous final state dispersion can be related to a linear combination of the initial position/velocity state dispersion δx_0 and a single impulsive maneuver Δv_0 at the nominal initial time t_0 .

$$\delta x_f = \phi_{f,0}(\delta x_0 + B\Delta v_0), \quad B_{6 \times 3} = \begin{bmatrix} 0 \\ I \end{bmatrix} \quad (7)$$

where the notation $\phi_{b,a}$ denotes the state-transition matrix from t_a to t_b . Substituting this into Eq. 6 produces

$$\Psi_{x,f} [\phi_{f,0}(\delta x_0 + B\Delta v_0) + \dot{x}_f^* \delta t_f] = 0 \quad (8)$$

or in a more compact form

$$\mathcal{M}\delta u = \mathcal{N}\delta x_0 \quad (9)$$

where

$$\delta u = \begin{bmatrix} \Delta v_0 \\ \delta t_f \end{bmatrix} \quad (10)$$

$$\mathcal{M} = \left\{ \Psi_{x,f} \begin{bmatrix} \phi_{f,0}B & \dot{x}_f^* \end{bmatrix} \right\}_{m \times 4} \quad (11)$$

and

$$\mathcal{N} = -[\Psi_{x,f} \phi_{f,0}]_{m \times 6} \quad (12)$$

These equations represents m constraints in $n = 4$ unknown controls, Δv_0 and δt_f . For fixed final-time problems, the fourth column of \mathcal{M} is removed.

Single Maneuver With Arbitrary Number of Constraints at Multiple Fixed or Variable Final Times

The previous section had only one set of constraints at a single fixed or variable final time. In this section let $\psi_i(x_{c_i}) = 0$ represent p_i nonlinear constraints at multiple variable times $t_{c_i}^* + \delta t_{c_i}$, for $i = 1, 2, \dots, r$, where δt_{c_i} represent r control parameters to be determined. The inertial position and velocity state vectors x_{c_i} , at variable times $t_{c_i}^* + \delta t_{c_i}$, must satisfy the constraints, $\psi_i(x_{c_i}) = 0$, and the nominal state vectors $x_{c_i}^*$ must also satisfy these constraints at the nominal times $t_{c_i}^*$, i.e., $\psi_i(x_{c_i}^*) = 0$. The r sets of constraints can be written as

$$\psi_1(x_{c_1}) = 0, \quad \psi_2(x_{c_2}) = 0, \quad \dots, \quad \psi_r(x_{c_r}) = 0$$

where each set of constraints ψ_i consists of p_i scalar constraints. The total number of constraints is $m = \sum_{i=1}^r p_i$.

If the non-contemporaneous state x_{c_i} is given by $x_{c_i} = x_{c_i}^* + \delta x_{c_i} + \dot{x}_{c_i}^* \delta t_{c_i}$, the p_i nonlinear constraints $\psi_i(x_{c_i})$ can be linearized about their respective nominal position and velocity state vectors $x_{c_i}^*$ to produce

$$\Psi_{x,c_1}(\delta x_{c_1} + \dot{x}_{c_1}^* \delta t_{c_1}) = 0, \quad \Psi_{x,c_2}(\delta x_{c_2} + \dot{x}_{c_2}^* \delta t_{c_2}) = 0, \quad \dots, \quad \Psi_{x,c_r}(\delta x_{c_r} + \dot{x}_{c_r}^* \delta t_{c_r}) = 0$$

where it is assumed that the reference trajectory also satisfies the constraint sets, $\psi_i(x_{c_i}^*) = 0$, $i = 1, 2, \dots, r$.

Utilizing linearized discrete-time dynamics, the contemporaneous state dispersion δx_{c_i} at time t_{c_i} can be related to a linear combination of the initial position/velocity state dispersion δx_0 and a single impulsive maneuver Δv_0 at the nominal initial time t_0 .

$$\delta x_{c_i} = \phi_{c_i,0}(\delta x_0 + B\Delta v_0), \quad B_{6 \times 3} = \begin{bmatrix} 0 \\ I \end{bmatrix}$$

Substituting the dispersion δx_i into the above $m = \sum_{i=1}^{n_p} p_i$ linearized constraints produces

$$\Psi_{x,c_1} [\phi_{c_1,0}(\delta x_0 + B\Delta v_0) + \dot{x}_{c_1}^* \delta t_{c_1}] = 0$$

$$\Psi_{x,c_2} [\phi_{c_2,0}(\delta x_0 + B\Delta v_0) + \dot{x}_{c_2}^* \delta t_{c_2}] = 0$$

$$\vdots$$

$$\Psi_{x,c_r} [\phi_{c_r,0}(\delta x_0 + B\Delta v_0) + \dot{x}_{c_r}^* \delta t_{c_r}] = 0$$

Rearranging produces

$$\Psi_{x,c_1} \phi_{c_1,0} B \Delta v_0 + \Psi_{x,c_1} \dot{x}_{c_1}^* \delta t_1 = -\Psi_{x,c_1} \phi_{c_1,0} \delta x_0$$

$$\Psi_{x,c_2} \phi_{c_2,0} B \Delta v_0 + \Psi_{x,c_2} \dot{x}_{c_2}^* \delta t_{c_2} = -\Psi_{x,c_2} \phi_{c_2,0} \delta x_0$$

$$\vdots$$

$$\Psi_{x,c_r} \phi_{c_r,0} B \Delta v_0 + \Psi_{x,c_r} \dot{x}_{c_r}^* \delta t_{c_r} = -\Psi_{x,c_r} \phi_{c_r,0} \delta x_0$$

which can be written in the compact form

$$\mathcal{M} \delta u = \mathcal{N} \delta x_0 \quad (13)$$

where

$$\delta u = \begin{bmatrix} \Delta v_0 \\ \delta T \end{bmatrix} \quad (14)$$

$$\mathcal{M} = \Psi \begin{bmatrix} \Phi B & \dot{\mathcal{X}} \end{bmatrix} \quad (15)$$

$$\Phi = \begin{bmatrix} \phi_{c_1,0} \\ \phi_{c_2,0} \\ \phi_{c_3,0} \\ \vdots \\ \phi_{c_r,0} \end{bmatrix}_{6r \times 6}, \mathcal{N} = - \begin{bmatrix} \Psi_{x,c_1} \Phi_{c_1,0} \\ \Psi_{x,c_2} \Phi_{c_2,0} \\ \vdots \\ \Psi_{x,c_r} \Phi_{c_r,0} \end{bmatrix}_{m \times 6}, \delta T = \begin{bmatrix} \delta t_{c_1} \\ \delta t_{c_2} \\ \vdots \\ \delta t_{c_r} \end{bmatrix}_{r \times 1} \quad (16)$$

$$\Psi = \begin{bmatrix} \Psi_{x,c_1} & 0 & \cdots & 0 \\ 0 & \Psi_{x,c_2} & \cdots & 0 \\ \vdots & \vdots & \ddots & \vdots \\ 0 & 0 & \cdots & \Psi_{x,c_n} \end{bmatrix}_{m \times 6r}, \dot{\mathcal{X}} = \begin{bmatrix} \dot{x}_{c_1}^* & 0 & \cdots & 0 \\ 0 & \dot{x}_{c_2}^* & \cdots & 0 \\ \vdots & \vdots & \ddots & \vdots \\ 0 & 0 & \cdots & \dot{x}_{c_r}^* \end{bmatrix}_{6r \times r} \quad (17)$$

These equations represents $m \geq r$ constraints (at least one scalar constraint at each of the r variable constraint times t_{c_i}) and $3 + r$ unknowns (the Δv_0 vector and the r time variations, δt_{c_i}). For fixed final-time problems $\dot{\mathcal{X}}$ can be removed leaving $\mathcal{M} = \Psi \Phi B$.

Multiple Maneuvers With Arbitrary Number of Constraints at Multiple Fixed or Variable Final Times

The previous section introduced an arbitrary number of sets of constraints at multiple variable times. The same constraints will be applied here, but with the addition of multiple maneuvers Δv_j at fixed maneuver times, $t_{\Delta v_j}$, $j = 1, 2, \dots, q$, that need to be solved for.

The r sets of linearized constraints are repeated here for convenience.

$$\Psi_{x,c_1} (\delta x_{c_1} + \dot{x}_{c_1}^* \delta t_{c_1}) = 0$$

$$\Psi_{x,c_2}(\delta x_{c_2} + \dot{x}_{c_2}^* \delta t_{c_2}) = 0$$

⋮

$$\Psi_{x,c_r}(\delta x_{c_r} + \dot{x}_{c_r}^* \delta t_{c_r}) = 0$$

where, as a reminder, each set of constraints ψ_i consists of p_i scalar constraints, and the total number of constraints is $m = \sum_{i=1}^r p_i$.

Utilizing linearized discrete-time dynamics, each of the contemporaneous state dispersions δx_{c_i} at time t_{c_i} is related to the initial state, δx_0 , and the maneuver impulses Δv_j at the fixed maneuver times, $t_{\Delta v_j}, j = 0, 1, \dots, q$. It is assumed there are q_1 maneuver impulses from t_0 to t_{c_1} , q_2 maneuver impulses from t_0 to t_{c_2} , etc., such that a total of $q = q_r$ maneuver impulses are allowed from t_0 to t_{c_r} . Using this maneuver numbering scheme, the state dispersions δx_{c_i} , at times $t_{c_i}, i = 1, 2, \dots, r$, are given by

$$\begin{aligned}\delta x_{c_1} &= \phi_{c_1,0} \delta x_0 + \sum_{j=0}^{q_1} \phi_{c_1,\Delta v_j} B \Delta v_j \\ \delta x_{c_2} &= \phi_{c_2,0} \delta x_0 + \sum_{j=0}^{q_2} \phi_{c_2,\Delta v_j} B \Delta v_j, \\ &\vdots \\ \delta x_{c_r} &= \phi_{c_r,0} \delta x_0 + \sum_{j=0}^{q=q_r} \phi_{c_r,\Delta v_j} B \Delta v_j,\end{aligned}$$

Substituting the above equations into the linearized constraints produces

$$\begin{aligned}\Psi_{x_{c_1}} \left[\phi_{c_1,0} \delta x_0 + \sum_{j=0}^{q_1} \phi_{c_1,\Delta v_j} B \Delta v_j + \dot{x}_{c_1}^* \delta t_{c_1} \right] &= 0 \\ \Psi_{x_{c_2}} \left[\phi_{c_2,0} \delta x_0 + \sum_{j=0}^{q_2} \phi_{c_2,\Delta v_j} B \Delta v_j + \dot{x}_{c_2}^* \delta t_{c_2} \right] &= 0 \\ &\vdots \\ \Psi_{x_{c_r}} \left[\phi_{c_r,0} \delta x_0 + \sum_{j=0}^{q=q_r} \phi_{c_r,\Delta v_j} B \Delta v_j + \dot{x}_{c_r}^* \delta t_{c_r} \right] &= 0\end{aligned}$$

where the notation $\phi_{c_r,\Delta v_j}$ denotes the state-transition matrix from t_{c_r} to $t_{\Delta v_j}$. Rearranging

$$\begin{aligned}\Psi_{x_{c_1}} \left[\sum_{j=0}^{q_1} \phi_{c_1,\Delta v_j} B \Delta v_j + \dot{x}_{c_1}^* \delta t_{c_1} \right] &= -\Psi_{x_{c_1}} \phi_{c_1,0} \delta x_0 \\ \Psi_{x_{c_2}} \left[\sum_{j=0}^{q_2} \phi_{c_2,\Delta v_j} B \Delta v_j + \dot{x}_{c_2}^* \delta t_{c_2} \right] &= -\Psi_{x_{c_2}} \phi_{c_2,0} \delta x_0\end{aligned}$$

$$\Psi_{x_{cr}} \left[\sum_{j=0}^{q=q_r} \phi_{c_r, \Delta v_j} B \Delta v_j + \dot{x}_{cr}^* \delta t_{cr} \right] = -\Psi_{x_{cr}} \phi_{c_r, 0} \delta x_0$$

or in a more compact form

$$\mathcal{M} \delta u = \mathcal{N} \delta x_0 \quad (18)$$

where

$$\delta u = \begin{bmatrix} \Delta V \\ \delta T \end{bmatrix} \quad (19)$$

$$\mathcal{M} = \Psi \begin{bmatrix} \Phi_q \mathcal{B} & \dot{\mathcal{X}} \end{bmatrix} \quad (20)$$

$$\Delta V = \begin{bmatrix} \Delta v_0 \\ \Delta v_1 \\ \vdots \\ \Delta v_q \end{bmatrix}_{3q \times 1}, \delta T = \begin{bmatrix} \delta t_{c_1} \\ \delta t_{c_2} \\ \vdots \\ \delta t_{c_r} \end{bmatrix}_{r \times 1}, \mathcal{N} = - \begin{bmatrix} \Psi_{x_{c_1}} \phi_{c_1, 0} \\ \Psi_{x_{c_2}} \phi_{c_2, 0} \\ \vdots \\ \Psi_{x_{c_r}} \phi_{c_r, 0} \end{bmatrix}_{m \times 6} \quad (21)$$

$$\Psi = \begin{bmatrix} \Psi_{x_{c_1}} & 0 & \cdots & 0 \\ 0 & \Psi_{x_{c_2}} & \cdots & 0 \\ \vdots & \vdots & \ddots & \vdots \\ 0 & 0 & \cdots & \Psi_{x_{c_n}} \end{bmatrix}_{m \times 6r}, \mathcal{B} = \begin{bmatrix} B & 0 & \cdots & 0 \\ 0 & B & \cdots & 0 \\ \vdots & \vdots & \ddots & \vdots \\ 0 & 0 & \cdots & B \end{bmatrix}_{6q \times 3q} \quad (22)$$

$$\Phi_q = \begin{bmatrix} \phi_{c_1, \Delta v_0} & \cdots & \phi_{c_1, \Delta v_{q_1}} & 0 & 0 & 0 & 0 & \cdots & 0 \\ \phi_{c_2, \Delta v_0} & \cdots & \phi_{c_2, \Delta v_{q_1}} & \cdots & \phi_{c_2, \Delta v_{q_2}} & 0 & 0 & \cdots & 0 \\ \phi_{c_3, \Delta v_0} & \cdots & \phi_{c_3, \Delta v_{q_1}} & \cdots & \phi_{c_3, \Delta v_{q_2}} & \cdots & \phi_{c_3, \Delta v_{q_3}} & \cdots & 0 \\ \vdots & \ddots & \vdots \\ \phi_{c_r, \Delta v_0} & \cdots & \phi_{c_r, \Delta v_{q_1}} & \cdots & \phi_{c_r, \Delta v_{q_2}} & \cdots & \phi_{c_r, \Delta v_{q_3}} & \cdots & \phi_{c_r, \Delta v_{q=n}} \end{bmatrix}_{6r \times 6q} \quad (23)$$

$$\dot{\mathcal{X}} = \begin{bmatrix} \dot{x}_{c_1}^* & 0 & \cdots & 0 \\ 0 & \dot{x}_{c_2}^* & \cdots & 0 \\ \vdots & \vdots & \ddots & \vdots \\ 0 & 0 & \cdots & \dot{x}_{c_r}^* \end{bmatrix}_{6r \times r} \quad (24)$$

These equations represents $m \geq r$ constraints (at least one scalar constraint at each of the r variable constraint times t_{ci}) and $3q + r$ unknowns (q Δv vectors and the r time variations, δt_{ci}). For fixed final-time problems \dot{X} can be removed leaving $\mathcal{M} = \Psi \Phi_q \mathcal{B}$.

DERIVATION OF A LINEAR FINITE-BURN TARGETING ALGORITHM

The objective of this section is to derive a linear finite-burn targeting algorithm that determines the values of $n \leq 7$ controls to achieve a set of m constraints at a variable final time. First, the linearized powered-flight equations of motion are used to derive a set of linear algebraic equations that relate initial trajectory dispersion and control perturbations and to position and velocity dispersion at the end of powered flight. The controls include thrust direction (2), thrust turning rate (2),

engine ignition time (1), and engine cutoff time (1). Next, a post-engine-cutoff coasting arc is introduced, and the associated linearized equations of motion are used to derive a set of linear algebraic equations that relate dispersion at the end of powered-flight to dispersion at the end of a variable duration coasting arc. The duration of the coasting arc is the 7th and final control in this problem. Lastly, a set of m nonlinear constraints on position and velocity at the end of the coasting arc is introduced and linearized. Combining all of the above elements results in a set of m equations and $n = 7$ unknown controls. These equations are then used to determine the n control perturbations that will achieve the final m constraints.

Powered-Flight Dynamics

The nonlinear powered-flight dynamics are written in terms of the inertial position $r(t)$ and velocity $v(t)$, the mass of the vehicle $m(t)$, the thrust magnitude $T(t)$, the thrust efficiency $\alpha = \text{constant}$ (defined as one divided by the equivalent engine exhaust velocity), and the thrust direction $\lambda(t)_T$. The relevant nonlinear differential equations are

$$\dot{r} = v \quad (25)$$

$$\dot{v} = g(r) + \frac{T}{m} \frac{\lambda_T}{\|\lambda_T\|} \quad (26)$$

$$\dot{m} = -T\alpha \quad (27)$$

$$\dot{\alpha} = 0 \quad (28)$$

If the nominal powered-flight trajectory beginning at time t_{tig}^* is defined by $r^*(t)$, $v^*(t)$, $m^*(t)$, α^* , and the nominal control is defined by $\lambda_T^*(t)$, the above equations can be linearized about the nominal values where the trajectory dispersions are given by $\delta r(t)$, $\delta v(t)$, $\delta m(t)$, $\delta \alpha(t)$, and the control perturbations are $\delta \lambda_T(t) = \delta \lambda + \delta \gamma(t - t_{tig}^*)$, where $\delta \lambda$, and $\delta \gamma$ are constants. The associated linearized differential equations are then given by

$$\dot{\delta r} = \delta v \quad (29)$$

$$\dot{\delta v} = G_r \delta r + M \delta m + \Lambda \delta \lambda + \Gamma \delta \gamma \quad (30)$$

$$\dot{\delta m} = -T \delta \alpha \quad (31)$$

$$\dot{\delta \alpha} = 0 \quad (32)$$

$$\dot{\delta \lambda} = 0 \quad (33)$$

$$\dot{\delta \gamma} = 0 \quad (34)$$

where

$$G_r = \left. \frac{\partial \dot{v}}{\partial r} \right|_* = \left. \frac{\partial g(r)}{\partial r} \right|_* \quad (35)$$

$$M = \left. \frac{\partial \dot{v}}{\partial m} \right|_* = -\frac{T}{m^2} \frac{\lambda^*}{\|\lambda^*\|} \quad (36)$$

$$\Lambda = \left. \frac{\partial \dot{v}}{\partial \lambda} \right|_* = \frac{T}{m} \frac{1}{\|\lambda^*\|} \left[I - \frac{\lambda^*}{\|\lambda^*\|} \frac{\lambda^{*T}}{\|\lambda^*\|} \right] \quad (37)$$

$$\Gamma = \left. \frac{\partial \dot{v}}{\partial \gamma} \right|_* = \Lambda(t - t_{tig}^*) \quad (38)$$

Although the trajectory dispersions and control perturbations are assumed to be small, there are generally no constraints on them. However, the initial thrust direction perturbation $\delta\lambda$ is required to be perpendicular to the nominal initial thrust $\lambda_{T,tig}^* = \lambda_T^*(t_{tig}^*)$. To enforce this constraint, the perturbation $\delta\lambda$ is written as

$$\delta\lambda = \delta c_1 \hat{\lambda}_{\perp 1}^* + \delta c_2 \hat{\lambda}_{\perp 2}^* \quad (39)$$

$$\delta\lambda = \begin{bmatrix} \hat{\lambda}_{\perp 1}^* & \hat{\lambda}_{\perp 2}^* \end{bmatrix} \begin{bmatrix} \delta c_1 \\ \delta c_2 \end{bmatrix} \quad (40)$$

$$\delta\lambda = L\delta c \quad (41)$$

where

$$\hat{\lambda}_{\perp 1}^* = \frac{\hat{\lambda}_{T,0}^* \times \hat{i}_z}{\|\hat{\lambda}_{T,0}^* \times \hat{i}_z\|} \quad (42)$$

$$\hat{\lambda}_{\perp 2}^* = \frac{\hat{\lambda}_{T,0}^* \times \hat{\lambda}_{\perp 1}^*}{\|\hat{\lambda}_{T,0}^* \times \hat{\lambda}_{\perp 1}^*\|} \quad (43)$$

Similarly, the turning rate perturbation $\delta\gamma$ is also assumed to be perpendicular to the initial nominal thrust direction.

$$\delta\gamma = \delta g_1 \hat{\lambda}_{\perp 1}^* + \delta g_2 \hat{\lambda}_{\perp 2}^* \quad (44)$$

$$\delta\gamma = \begin{bmatrix} \hat{\lambda}_{\perp 1}^* & \hat{\lambda}_{\perp 2}^* \end{bmatrix} \begin{bmatrix} \delta g_1 \\ \delta g_2 \end{bmatrix} \quad (45)$$

$$\delta\gamma = L\delta g \quad (46)$$

Using this formulation for the thrust vector perturbations, the state vector perturbation δX , consisting of trajectory dispersions and control perturbations, is given by

$$\delta X = [\delta r, \delta v, \delta m, \delta\alpha, \delta c, \delta g]^T \quad (47)$$

and the associated linearized differential equations are $\dot{\delta X} = F(t)\delta X$, or

$$\dot{\delta r} = \delta v \quad (48)$$

$$\dot{\delta v} = G_r \delta r + M \delta m + \Lambda L \delta c + \Gamma L \delta g \quad (49)$$

$$\dot{\delta m} = -T \delta\alpha \quad (50)$$

$$\dot{\delta\alpha} = 0 \quad (51)$$

$$\dot{\delta c} = 0 \quad (52)$$

$$\dot{\delta g} = 0 \quad (53)$$

where the Jacobian $F(t)$ is given by

$$F(t) = \begin{bmatrix} 0_{3 \times 3} & I_{3 \times 3} & 0_{3 \times 1} & 0_{3 \times 1} & 0_{3 \times 2} & 0_{3 \times 2} \\ G_r & 0_{3 \times 3} & M & 0_{3 \times 1} & \Lambda L & \Gamma L \\ 0_{1 \times 3} & 0_{1 \times 3} & 0 & -T & 0_{1 \times 2} & 0_{1 \times 2} \\ 0_{1 \times 3} & 0_{1 \times 3} & 0 & 0 & 0_{1 \times 2} & 0_{1 \times 2} \\ 0_{2 \times 3} & 0_{2 \times 3} & 0_{2 \times 1} & 0_{2 \times 1} & 0_{2 \times 2} & 0_{2 \times 2} \\ 0_{2 \times 3} & 0_{2 \times 3} & 0_{2 \times 1} & 0_{2 \times 1} & 0_{2 \times 2} & 0_{2 \times 2} \end{bmatrix} \quad (54)$$

The state dispersion $\delta X(t_{co}^*)$ at the nominal engine cutoff time t_{co}^* due to the dispersion $\delta X(t_{tig}^*)$ at the nominal time of ignition t_{tig}^* and a variable engine ignition time, δt_{tig} , is given by

$$\delta X(t_{co}^*) = \Phi(t_{co}^*, t_{tig}^* + \delta t_{tig}) \left[\delta X(t_{tig}^*) + \dot{X}_{tig}^* \delta t_{tig} \right] \quad (55)$$

where \dot{X}_{tig}^* are the state derivatives for coasting flight prior to engine ignition. Discarding second-order terms, Eq. 55 becomes

$$\delta X(t_{co}^*) = \Phi(t_{co}^*, t_{tig}^*) \left[\delta X(t_{tig}^*) + \dot{X}_{tig}^* \delta t_{tig} \right] \quad (56)$$

and when the engine cut-off time is allowed to vary, the state dispersion $\delta X(t_{co}^* + \delta t_{co})$ at engine cut-off $t_0^* + \delta t_0$ is

$$\delta X(t_{co}^* + \delta t_{co}) = \Phi(t_{co}^*, t_{tig}^*) \left[\delta X(t_{tig}^*) + \dot{X}_{tig}^* \delta t_{tig} \right] + \dot{X}_{co}^* \delta t_{co} \quad (57)$$

where \dot{X}_{co}^* are the state derivatives for powered-flight, and once again second-order terms have been discarded.

Lastly, if the state associated with the position and velocity is denoted by

$$x = \begin{bmatrix} r \\ v \end{bmatrix} \quad (58)$$

the state transition matrix can be partitioned and written as

$$\Phi(t_{co}^*, t_{tig}^*) = \begin{bmatrix} \phi_{xx}(t_{co}^*, t_{tig}^*) & \phi_{xm}(t_{co}^*, t_{tig}^*) & \phi_{x\alpha}(t_{co}^*, t_{tig}^*) & \phi_{xc}(t_{co}^*, t_{tig}^*) & \phi_{xg}(t_{co}^*, t_{tig}^*) \\ 0_{1 \times 6} & 1 & -T(t_{co}^* - t_0^*) & 0_{1 \times 2} & 0_{1 \times 2} \\ 0_{1 \times 6} & 0 & 1 & 0_{1 \times 2} & 0_{1 \times 2} \\ 0_{2 \times 6} & 0_{2 \times 1} & 0_{2 \times 1} & I_{2 \times 2} & 0_{2 \times 2} \\ 0_{2 \times 6} & 0_{2 \times 1} & 0_{2 \times 1} & 0_{2 \times 2} & I_{2 \times 2} \end{bmatrix} \quad (59)$$

and the position/velocity state dispersion at a variable engine cutoff time is

$$\begin{aligned} \delta x(t_{co}^* + \delta t_{co}) = & \phi_{xx}(t_{co}^*, t_{tig}^*) [\delta x(t_{tig}^*) + \dot{x}_{tig}^* \delta t_{tig}] + \phi_{xm}(t_{co}^*, t_{tig}^*) \delta m_{tig} + \phi_{x\alpha}(t_{co}^*, t_{tig}^*) \delta \alpha + \\ & \phi_{xc}(t_{co}^*, t_{tig}^*) \delta c + \phi_{xg}(t_{co}^*, t_{tig}^*) \delta g + \dot{x}_{co}^* \delta t_{co} \end{aligned} \quad (60)$$

Coasting Flight Dynamics

The results of the previous section can be applied for coasting flight with zero thrust. In this case the state transition matrix from engine cutoff t_{co}^* to the final t_f^* can be partitioned and written as

$$\Phi(t_f^*, t_{co}^*) = \begin{bmatrix} \phi_{xx}(t_f^*, t_{co}^*) & 0_{6 \times 1} & 0_{6 \times 1} & 0_{6 \times 2} & 0_{6 \times 2} \\ 0_{1 \times 6} & 1 & 0 & 0_{1 \times 2} & 0_{1 \times 2} \\ 0_{1 \times 6} & 0 & 1 & 0_{1 \times 2} & 0_{1 \times 2} \\ 0_{2 \times 6} & 0_{2 \times 1} & 0_{2 \times 1} & I_{2 \times 2} & 0_{2 \times 2} \\ 0_{2 \times 6} & 0_{2 \times 1} & 0_{2 \times 1} & 0_{2 \times 2} & I_{2 \times 2} \end{bmatrix} \quad (61)$$

The state perturbation at the nominal final time t_f^* due to a state perturbation at the nominal engine cutoff t_{co}^* is

$$\delta x(t_f^*) = \phi_{xx}(t_f^*, t_{co}^*)\delta x(t_{co}^*) \quad (62)$$

When the engine cutoff time is allowed to vary, $t_{co}^* + \delta t_{co}$, the final state perturbation is

$$\delta x(t_f^*) = \phi_{xx}(t_f^*, t_{co}^* + \delta t_{co})\delta x(t_{co}^* + \delta t_{co}) \quad (63)$$

However, discarding second-order terms this simply becomes

$$\delta x(t_f^*) = \phi_{xx}(t_f^*, t_{co}^*)\delta x(t_{co}^* + \delta t_{co}) \quad (64)$$

and if the final time is allowed to vary, the final state perturbation is

$$\delta x(t_f^* + \delta t_f) = \phi_{xx}(t_f^*, t_{co}^*)\delta x(t_{co}^* + \delta t_{co}) + \dot{x}_f^*\delta t_f \quad (65)$$

where second-order terms have again been discarded.

Linearized Finite-Burn Variable Final-Time Targeting

Consider the nonlinear position/velocity constraint at the end of the coasting arc.

$$\Psi(x_f) = 0 \quad (66)$$

Linearizing about x_f^* and allowing for a variable final time $t_f^* + \delta t_f$ produces

$$\Psi(x_f^*) + \left. \frac{\partial \Psi}{\partial x_f} \right|_* \delta x(t_f^* + \delta t_f) = 0, \quad \text{where } \Psi(x_f^*) = 0 \quad (67)$$

or

$$\Psi_{x_f}[\delta x(t_f^* + \delta t_f)] = 0, \quad \text{where } \Psi_{x_f} = \left. \frac{\partial \Psi}{\partial x_f} \right|_* \quad (68)$$

The final state perturbation $\delta x(t_f^* + \delta t_f)$ in Eq. 68 is obtained by substituting Eq. 60 into Eq. 65

$$\begin{aligned} \delta x(t_f^* + \delta t_f) = & \phi_{xx}(t_f^*, t_{co}^*) \{ \phi_{xx}(t_{co}^*, t_{tig}^*) [\delta x(t_{tig}^*) + \dot{x}_{tig}^* \delta t_{tig}] + \phi_{xm}(t_{co}^*, t_{tig}^*) \delta m_{tig} + \\ & + \phi_{x\alpha}(t_{co}^*, t_{tig}^*) \delta \alpha + \phi_{xc}(t_{co}^*, t_{tig}^*) \delta c + \phi_{xg}(t_{co}^*, t_{tig}^*) \delta g + \dot{x}_{co}^* \delta t_{co} \} + \dot{x}_f^* \delta t_f \end{aligned} \quad (69)$$

Substituting $\delta x(t_f^* + \delta t_f)$ into Eq. 68 produces

$$0 = \Psi_{x_f} \phi_{xx}(t_f^*, t_{co}^*) \{ \phi_{xx}(t_{co}^*, t_{tig}^*) [\delta x(t_{tig}^*) + \dot{x}_{tig}^* \delta t_{tig}] + \phi_{xm}(t_{co}^*, t_{tig}^*) \delta m_{tig} + \phi_{x\alpha}(t_{co}^*, t_{tig}^*) \delta \alpha + \\ \phi_{xc}(t_{co}^*, t_{tig}^*) \delta c + \phi_{xg}(t_{co}^*, t_{tig}^*) \delta g + \dot{x}_{co}^* \delta t_{co} \} + \Psi_{x_f} \dot{x}_f^* \delta t_f \quad (70)$$

Separating control terms from the initial state dispersion and rearranging, the above equation can be written as

$$\mathcal{M} \begin{bmatrix} \delta c \\ \delta g \\ \delta t_{tig} \\ \delta t_{co} \\ \delta t_f \end{bmatrix} = \mathcal{N} \begin{bmatrix} \delta x_{tgt} \\ \delta m_{tgt} \\ \delta \alpha \end{bmatrix} \quad (71)$$

where

$$\mathcal{M} = \begin{bmatrix} K\phi_{xc}(t_{co}^*, t_{tig}^*) & K\phi_{xg}(t_{co}^*, t_{tig}^*) & K\phi_{xx}(t_{co}^*, t_{tig}^*)\dot{x}_{tig}^* & K\dot{x}_{co}^* & \Psi_{x_f}\dot{x}_f^* \end{bmatrix} \quad (72)$$

$$\mathcal{N} = -K \begin{bmatrix} \phi_{xx}(t_{co}^*, t_{tig}^*) & \phi_{xm}(t_{co}^*, t_{tig}^*) & \phi_{x\alpha}(t_{co}^*, t_{tig}^*) \end{bmatrix} \quad (73)$$

$$K = \Psi_{x_f}\phi_{xx}(t_f^*, t_{co}^*) \quad (74)$$

Eq. 71 represents m constraint equations in 7 unknown controls, $\delta c = [\delta c_1, \delta c_2]^T$, $\delta g = [\delta g_1, \delta g_2]^T$, δt_0 , δt_{co} , and δt_f . When constraints are added or removed from the targeting problem, the corresponding rows of \mathcal{M} and \mathcal{N} are added or removed. If fewer controls are required, the corresponding columns of \mathcal{M} are removed.

Linearized Finite Burn Targeting Algorithm

Given the nominal values for the inertial position and velocity $r^*(t)$ and $v^*(t)$, the mass $m^*(t)$, the thrust magnitude $T(t)$, efficiency α^* , thrust direction $\lambda_T^*(t)$, and the nominal ignition and cutoff time of the finite burn, t_0^* and t_{co}^* , evaluate the Jacobian $F(t)$ in Eq. 54 from t_{tig} to t_{co}^* , using Eqs. 35-38.

Next, using the second order approximation for the powered flight state transition matrix from t_i to t_{i+1} ,

$$\Phi(t_{i+1}, t_i) = I + [F(t_i) + F(t_{i+1})]\frac{\Delta t}{2} + F(t_i)F(t_{i+1})\frac{\Delta t^2}{2} \quad (75)$$

compute the total transition matrix $\Phi(t_{co}^*, t_{tig}^*)$.

$$\Phi(t_{co}^*, t_{tig}^*) = \Phi(t_{co}^*, t_{co-1}) \dots \Phi(t_{i+1}, t_i) \dots \Phi(t_2, t_1) \Phi(t_1, t_{tig}^*) \quad (76)$$

After this, compute the Jacobian for coasting flight ($T(t) = 0$) from t_{co}^* to t_f^* and the associated state-transition matrix in Eq. 35 and extract the position/velocity state-transition matrix, $\phi_{xx}(t_f^*, t_{co}^*)$.

Next, compute the constraint partial derivative at the nominal final position and velocity Ψ_{x_f} , the position/velocity time derivatives at the nominal engine ignition time \dot{x}_{tig}^* , and cutoff time \dot{x}_{co}^* , and at the nominal final time, \dot{x}_f^* .

$$\Psi_{x_f} = \left. \frac{\partial \Psi}{\partial x_f} \right|_* \quad (77)$$

$$\dot{x}_{tig}^* = \begin{bmatrix} v_{tig}^* \\ g(r_{tig}^*) \end{bmatrix} \quad (78)$$

$$\dot{x}_{co}^* = \begin{bmatrix} v_{co}^* \\ g(r_{co}^*) + \frac{T^*}{m_{co}^*} \frac{\lambda_T^*}{\|\lambda_T^*\|} \end{bmatrix} \quad (79)$$

$$\dot{x}_f^* = \begin{bmatrix} v_f^* \\ g(r_f^*) \end{bmatrix} \quad (80)$$

Lastly, extract $\phi_{xx}(t_{co}^*, t_{tig}^*)$, $\phi_{xc}(t_{co}^*, t_{tig}^*)$, $\phi_{xm}(t_{co}^*, t_{tig}^*)$, and $\phi_{x\alpha}(t_{co}^*, t_{tig}^*)$ from $\Phi(t_{co}^*, t_{tig}^*)$ and compute the \mathcal{M} and \mathcal{N} matrices in Eqs. 72 and 73.

Once the the \mathcal{M} and \mathcal{N} matrices in Eqs. 72 and 73 have been computed, Eqs. 2-4 can be used to determine the control solutions depending on whether the problem well-defined, under-determined or over-determined. In all cases, the solution for the thrust direction is given by

$$\lambda_T(t) = \lambda_T^*(t) + \delta\lambda + \delta\gamma(t - t_{tig}^*) = \lambda_T^*(t) + L\delta c + L\delta g(t - t_{tig}^*) \quad (81)$$

where L is determined from Eqs. 40-41 and Eqs. 42-43.

FINITE-BURN ORBIT-TRANSFER DEMONSTRATION

This section explores the performance of finite-burn targeting using a linear covariance analysis tool. TA description of the implementation of finite-burn targeting in a linear covariance (LinCov) analysis is described in Appendix A.

The example presented here is a finite-burn orbital transfer. The spacecraft is initially in a near circular orbit. The thrust profile consists of a nominal initial direction and constant turn-rate. The engines are turned on at the nominal time-of-ignition (TIG) $t = 0$ sec and off at the nominal engine cut-off time, $t = 300$ sec. If the initial trajectory dispersions are zero, the nominal thrust profile will deliver the spacecraft to the desired final position and velocity.

When the initial dispersion are not zero, e.g., $\delta r=10$ km $1-\sigma$ /axis, $\delta v=100$ m/s $1-\sigma$ /axis, $\delta m= 2\%$ $1-\sigma$, and $\delta\alpha= 2\%$ $1-\sigma$, an uncorrected nominal thrust profile results in over 200 km $1-\sigma$ of final position dispersion and 0.4 km/s $1 - \sigma$ of final velocity dispersion. This is shown in Fig. 1.

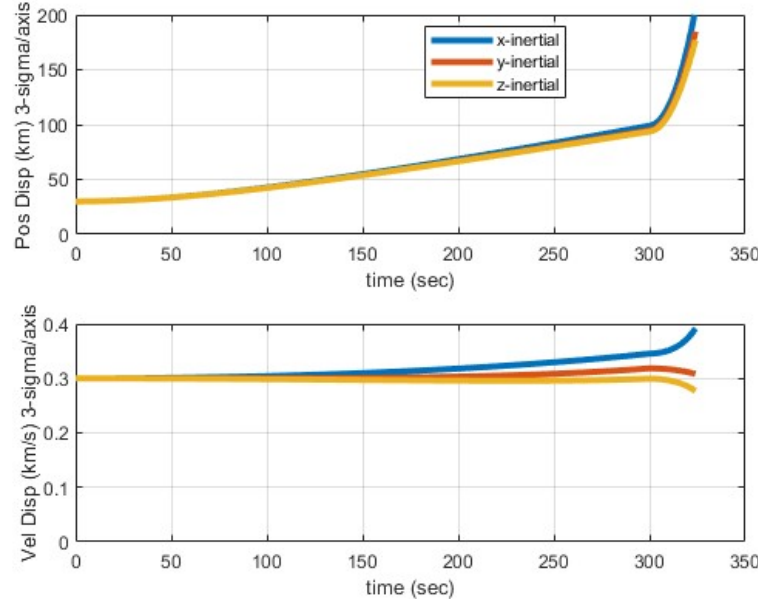


Figure 1. Position and velocity dispersion $1-\sigma$ without corrections to TIG, thrust direction, turn-rate, and engine cut-off time

However, when the finite-burn targeting is implemented and used to "correct" the initial thrust direction, turn-rate, TIG, and engine cut-off time, the final position and velocity dispersions are

reduced to zero as shown in Fig. 2. In this example, all of the 6 controls are "corrected" to achieve the final 6 position and velocity targets. The values of the corrections in this example are $\delta t_{tig} = 6.5$ sec $1-\sigma$, $\delta c = [4.5 \ 2.1]$ deg $1-\sigma$, $\delta g = [0.03 \ 0.01]$ deg/sec $1-\sigma$, and $\delta t_{co} = 3.0$ sec $1-\sigma$. The effect of TIG and cut-off corrections is seen in Fig. 2 as instantaneous changes to the position and velocity covariance at the nominal TIG and cut-off times.

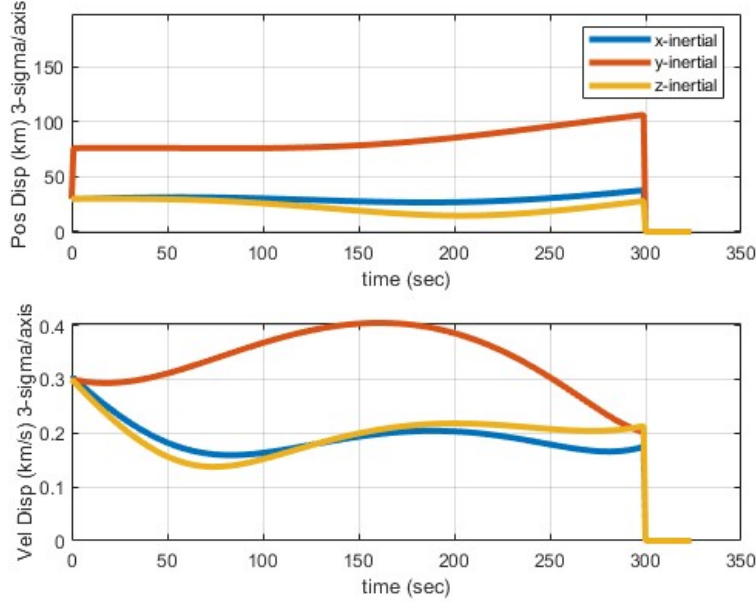


Figure 2. Position and velocity dispersion $1-\sigma$ with corrections to TIG, thrust direction, turn-rate, and engine cut-off time

CIS-LUNAR DEMONSTRATION

One key element to enable robust trajectory optimization is the ability to produce maneuver partials quickly and reliably from the various targeting algorithms. Currently, the nonlinear targeting algorithms for cis-lunar applications such as the Two-Level Targeter (TLT) are rather *slow*. The generalized linear targeting (GLT) has been developed to provide an alternate solution to the nonlinear targeting algorithms for analysis purposes. To demonstrate and validate the performance of GLT, a cislunar transfer scenario from low Earth orbit to low lunar orbit⁶ is utilized as shown in Figure 3. The test scenario starts shortly after the trans-lunar injection (TLI) burn and applies several arbitrary translational correction maneuvers (TCM) while attempting to comply with several targeting constraints at a specific time prior to lunar orbit insertion (LOI).

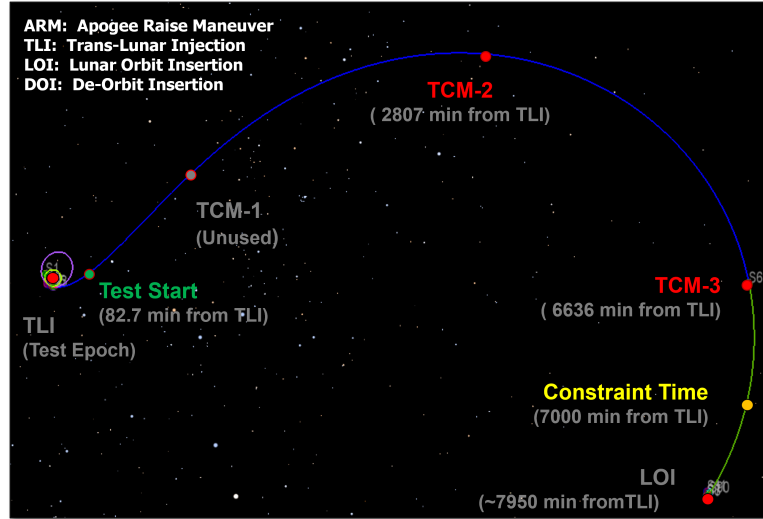


Figure 3. Nominal cislunar trajectory with arbitrary trajectory correction maneuver (TCM) locations

For the first demonstration case, the GLT is given targeting constraints in position and velocity magnitude at 7,000 minutes. TCM-1 is ignored for this case, leaving TCM-2 and TCM-3 to each be executed with the single maneuver formulation. Assuming only initial dispersions (no navigation errors, maneuver execution errors, or process noise), the results in Figure 4 show the trajectory dispersion for the position and velocity magnitude go to zero (see plots on right side of the figure), which is consistent with the prescribed targeting constraints.

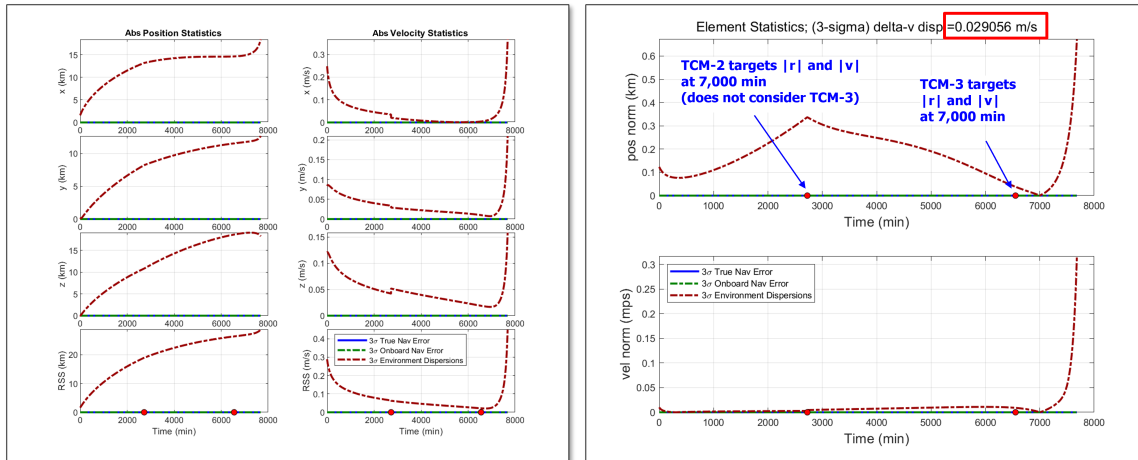


Figure 4. Case 1 and Constraint Set 1: Individual Dispersion Only, Individual Targeting

Generalized Linear Targeting Comparison to Two-Level Targeter

Following initial evaluations of GLT, its LinCov performance was compared against TLT. For example, Figure 5 highlights a case where GLT is used to do point-to-point targeting using TCM-1, TCM-2, and TCM-3. In this configuration, TCM-1 and TCM-2 target position at the time of the next

maneuver while TCM-3 targets position at the final time. This same scenario is replicated using the TLT algorithm as shown in Figure 6. Two versions of this case are run for each targeting algorithm: one where initial dispersions are the only error source considered, and one where the full error and measurement model is used. For both cases, GLT and TLT display similar performance. In the first version, the results of the two algorithms are nearly identical. Conversely, in the second, GLT results in higher dispersions and Delta-V requirements than TLT, suggesting that GLT over-corrects in the presence of full error sources.

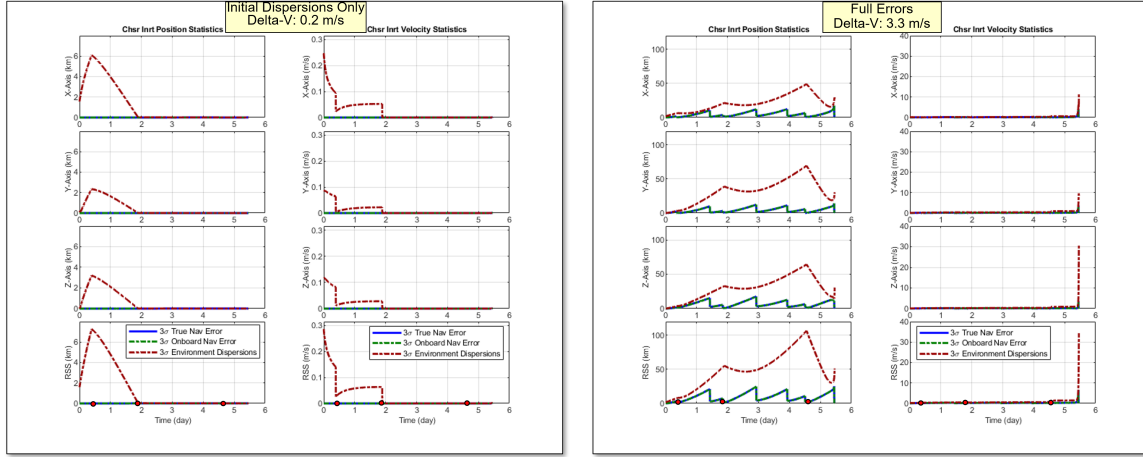


Figure 5. GLT and TLT Comparison: GLT Point-to-Point Targeting

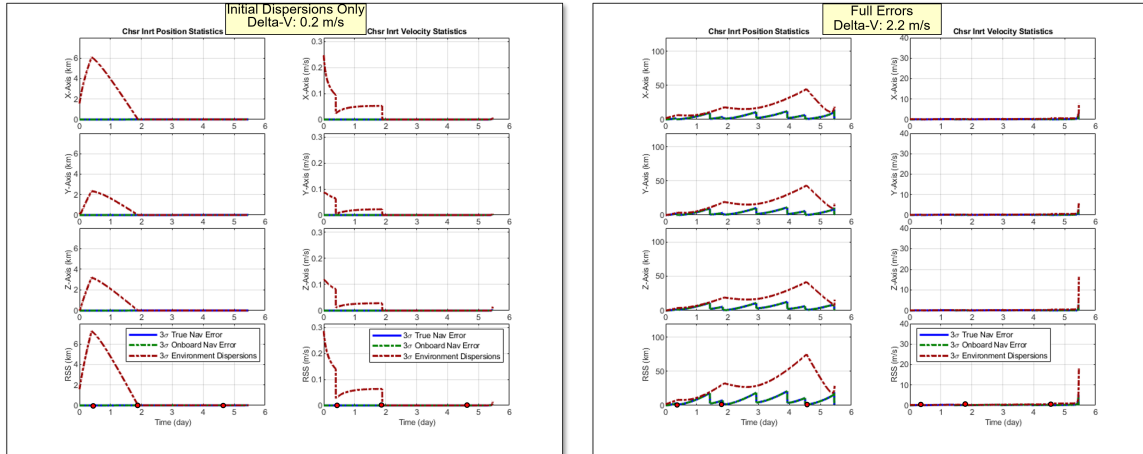


Figure 6. GLT and TLT Comparison: TLT Point-to-Point Targeting

CONCLUSION

In this paper, a set of generalized linear targeting algorithms that mimics many of the properties of the TLT has been derived. The generalized algorithms can handle single or multiple impulsive maneuvers, with multiple constraints at multiple fixed or variable times. A linear targeting algorithm for finite burn maneuvers was also derived. The generalized linear targeting algorithms are

exceptionally fast and easy to implement in Monte Carlo analysis, linear covariance (LinCov) analysis, and robust optimal trajectory design. Several examples validating the new algorithms were presented.

REFERENCES

- [1] S. S. Harris, C. M. Spreen, M. T. Stoft, R. J. Frank, and R. J. Stewart, “Performance of the Two-Level Targeting Algorithm on Artemis I,” *AAS 23-056, AAS Guidance and Control Conference, Breckenridge, CO, February 2023*, 2023.
- [2] S. K. Scarritt, T. Fill, and S. Robinson, “Advances in Orion’s On-Orbit Guidance and Targeting System Architecture,” *AAS Guidance Navigation and Control Conference*, No. JSC-CN-32859, 2015.
- [3] B. G. Marchand, M. W. Weeks, C. W. Smith, and S. Scarritt, “Onboard autonomous targeting for the trans-earth phase of orion,” *Journal of Guidance, Control, and Dynamics*, Vol. 33, No. 3, 2010, pp. 943–956.
- [4] S. K. Scarritt, *A self-contained guidance and targeting algorithm for spacecraft applications*. PhD thesis, 2012.
- [5] D. G. Hull, *Optimal control theory for applications*. Springer Science & Business Media, 2013.
- [6] D. Geller, D. Woffinden, and S. Bieniawski, “Sensitivity of Optimal Midcourse Correction Scheduling for Robust Cislunar Trajectory Design,” *AAS Guidance, Navigation, and Control Conference*, 2023, pp. AAS 23-061.
- [7] D. K. Geller, “Linear covariance techniques for orbital rendezvous analysis and autonomous onboard mission planning,” *Journal of Guidance, Control, and Dynamics*, Vol. 29, No. 6, 2006, pp. 1404–1414.

APPENDIX A - COVARIANCE ANALYSIS FOR FINITE BURNS

The implementation of the above finite-burn maneuver targeting algorithm for linear covariance (LinCov) analysis is presented in this section. Navigation errors, maneuver execution errors, and random disturbances are assumed to be zero. Only the essential aspects of the finite-burn maneuver targeting algorithm on the LinCov dispersion covariance will be considered. In particular, the equations relating the variable engine ignition time δt_{tig} , cutoff time δt_{co} , and constraint time δt_c , on the LinCov dispersion covariance are developed. This development can be expanded to include navigation errors, maneuver execution errors, and random disturbances if a full closed-loop LinCov analysis⁷ is needed.

Define the LinCov dispersion state vector to consist of trajectory dispersions δr , δv , δm , and $\delta \alpha$, and control perturbations δc , δg , as defined in Eq. 47. Augment this state with the variable times δt_{tig} , δt_{co} and δt_c , i.e., $\delta X = [\delta r, \delta v, \delta m, \delta \alpha, \delta c, \delta g, \delta t_{tig}, \delta t_{co}, \delta t_c]^T$, where $\dot{\delta t}_{tig} = \dot{\delta t}_{co} = \dot{\delta t}_c = 0$. It is assumed that the STM for this state vector is available and denoted by $\Phi_C(t_2, t_1)$ for coasting flight, and $\Phi_P(t_2, t_1)$ for powered flight, for arbitrary times t_1, t_2 .

At the nominal initial time t_0^* , the initial LinCov state dispersion vector is given by $\delta X_0 = [\delta r_0, \delta v_0, \delta m_0, \delta \alpha_0, 0_{7 \times 1}]^T$, and the initial LinCov dispersion covariance is

$$P_0 = \begin{bmatrix} P_{r_0 r_0} & P_{r_0 v_0} & 0_{3 \times 1} & 0_{3 \times 1} & 0_{3 \times 7} \\ P_{v_0 r_0} & P_{v_0 v_0} & 0_{3 \times 1} & 0_{3 \times 1} & 0_{3 \times 7} \\ 0_{1 \times 3} & 0_{1 \times 3} & \sigma_{m_0}^2 & 0 & 0_{1 \times 7} \\ 0_{1 \times 3} & 0_{1 \times 3} & 0 & \sigma_{\alpha_0}^2 & 0_{1 \times 7} \\ 0_{7 \times 3} & 0_{7 \times 3} & 0_{7 \times 1} & 0_{7 \times 1} & 0_{7 \times 7} \end{bmatrix} \quad (82)$$

This initial state dispersion and covariance is propagated forward up to the time just before the targeting algorithm is called according to

$$\delta X_{tgt}^- = \Phi_C(t_{tgt}^*, t_0^*) \delta X_0 \quad (83)$$

$$P_{tgt}^- = \Phi_C(t_{tgt}^*, t_0^*) P_0 \Phi_C(t_{tgt}^*, t_0^*)^T \quad (84)$$

When the targeting algorithm is executed at time t_{tgt}^* , the dispersion in the controls, δc , δg , and variable times δt_{tig} , δt_{co} , and δt_c , are computed and given by

$$\begin{bmatrix} \delta c \\ \delta g \\ \delta t_{tig} \\ \delta t_{co} \\ \delta t_c \end{bmatrix} = \mathcal{P}_u \begin{bmatrix} \delta r_{tgt} \\ \delta v_{tgt} \\ \delta m_{tgt} \\ \delta \alpha_{tgt} \end{bmatrix} \quad (85)$$

where the partial derivative of the control perturbations and variable times with respect to the trajectory dispersions, \mathcal{P}_u , at t_{tgt}^* , are determined from either Eq. 2, $\mathcal{P}_u = \mathcal{M}^{-1}\mathcal{N}$, or Eq. 3, $\mathcal{P}_u = (\mathcal{M}^T W_\psi \mathcal{M})^{-1} \mathcal{M}^T W_\psi \mathcal{N}$, or Eq. 4, $\mathcal{P}_u = (W_c \mathcal{M}^T (\mathcal{M} W_c \mathcal{M}^T)^{-1} \mathcal{N}$, and where the matrices \mathcal{M} and \mathcal{N} are given by Eqs. 72 and 73.

Based on Eq. 85, the effect of the targeting algorithm is to “correct” the LinCov state dispersion and covariance at time t_{tgt}^* according to

$$\delta X_{tgt}^+ = \begin{bmatrix} I_{8 \times 8} & 0_{8 \times 7} \\ \mathcal{P}_u & 0_{7 \times 7} \end{bmatrix} \delta X_{tgt}^- = \Phi_{tgt} \delta X_{tgt}^- \quad (86)$$

$$P_{tgt}^+ = \Phi_{tgt} P_{tgt}^- \Phi_{tgt}^T$$

where the single subscript on Φ_{tgt} denotes an instantaneous state-correction matrix used to correct δX_{tgt} and P_{tgt} at time t_{tgt}^* .

Next, the state dispersion and covariance are propagated to the nominal engine ignition time t_{tig}^*

$$\delta X_{tig}^- = \Phi_C(t_{tig}^*, t_{tgt}^*) \delta X_{tgt}^+ \quad (87)$$

$$P_{tig}^- = \Phi_C(t_{tig}^*, t_{tgt}^*) P_{tgt}^+ \Phi_C(t_{tig}^*, t_{tgt}^*)^T \quad (88)$$

At the nominal engine ignition time t_{tig}^* , the effect of the variable engine ignition time δt_{tig} on the state dispersion is

$$\delta X_{tig}^+ = \delta X_{tig}^- + \dot{X}_{tig}^* \delta t_{tig} \quad (89)$$

$$= \left[I + \dot{X}_{tig}^* \mathcal{P}_{\delta t_{tig}} \right] \delta X_{tig}^- \quad (90)$$

$$= \Phi_{tig} \delta X_{tig}^- \quad (91)$$

where $\mathcal{P}_{\delta t_{tig}}$ is the partial derivative of δt_{tig} with respect to the LinCov state dispersion vector δX , \dot{X}_{tig}^* is the nominal state time-derivative just prior to engine ignition, and $\Phi_{tig} = I + \dot{X}_{tig}^* \mathcal{P}_{\delta t_{tig}}$ denotes an instantaneous state-correction matrix at time t_{tig}^* . Using the equation above, the effect of the variable engine ignition time δt_{tig} on the LinCov dispersion covariance is

$$P_{tig}^+ = \Phi_{tig} P_{tig}^- \Phi_{tig}^T \quad (92)$$

and, once powered flight begins, the state dispersion and covariance are propagated to the nominal engine cutoff time according to

$$\delta X_{co}^- = \Phi_P(t_{co}^*, t_{tig}^*) \delta X_{tig}^+ \quad (93)$$

$$P_{co}^- = \Phi_P(t_{co}^*, t_{tig}^*) P_{tig}^+ \Phi_P(t_{co}^*, t_{tig}^*)^T \quad (94)$$

At the nominal engine cutoff time t_{co}^* , the effect of the variable engine cutoff time δ_{co} on the state dispersion is

$$\delta X_{co}^+ = \delta X_{co}^- + \dot{X}_{co}^* \delta t_{co} \quad (95)$$

$$= \left[I + \dot{X}_{co}^* \mathcal{P}_{\delta t_{co}} \right] \delta X_{co}^- \quad (96)$$

$$= \Phi_{co} \delta X_{co}^- \quad (97)$$

where $\mathcal{P}_{\delta t_{co}}$ is the partial derivative of δt_{co} with respect to the LinCov state dispersion vector δX , \dot{X}_{co}^* is the nominal state time-derivative just prior to engine shutdown, and $\Phi_{co} = I + \dot{X}_{co}^* \mathcal{P}_{\delta t_{co}}$ denotes an instantaneous state-correction matrix at time t_{co}^* . Using the equation above, the effect of the variable engine cutoff time δt_{co} on the LinCov dispersion covariance is

$$P_{co}^+ = \Phi_{co} P_{co}^- \Phi_{co}^T \quad (98)$$

At the end of powered-flight, coasting flight begins and the state dispersion and covariance are propagated to the nominal constraint time t_c^*

$$\delta X_c^- = \Phi_C(t_c^*, t_{co}^*) \delta X_{co}^+ \quad (99)$$

$$P_c^- = \Phi_C(t_c^*, t_{co}^*) P_{co}^+ \Phi_C(t_c^*, t_{co}^*)^T \quad (100)$$

Lastly the effect of the variable constraint time δt_c on the state dispersion and covariance is given by

$$\delta X_c^+ = \delta X_c^- + \dot{X}_c^* \delta t_c \quad (101)$$

$$= \left[I + \dot{X}_c^* \mathcal{P}_{\delta t_c} \right] \delta X_c^- \quad (102)$$

$$= \Phi_c \delta X_c^- \quad (103)$$

and

$$P_c^+ = \Phi_c P_c^- \Phi_c^T \quad (104)$$

and the state dispersion and covariance is then propagated to the nominal final time t_f^* according to

$$\delta X_f = \Phi_C(t_f^*, t_c^*) \delta X_c^+ \quad (105)$$

$$P_f = \Phi_C(t_f^*, t_c^*) P_c^+ \Phi_C(t_f^*, t_c^*)^T \quad (106)$$

APPENDIX B - COVARIANCE ANALYSIS FOR IMPULSIVE BURNS

The implementation of the above impulsive maneuver targeting algorithms for linear covariance (LinCov) analysis is discussed in this section. Navigation errors, maneuver execution errors, and random disturbances are assumed to be zero. Only the essential aspects of the above impulsive maneuver targeting algorithm on the LinCov dispersion covariance will be considered. In particular, the implementation of multiple impulsive Δv maneuvers and multiple variable constraint times in a LinCov dispersion analysis is developed. To limit the discussion, only two maneuvers at fixed times $t_{\Delta v_1}^*$, $t_{\Delta v_2}^*$ and two nominal constraint times $t_{c1}^* > t_{\Delta v_1}^*$, $t_{c2}^* > t_{\Delta v_2}^*$ will be considered. This

development can be expanded to include navigation errors, maneuver execution errors, and random disturbances if a full closed-loop LinCov analysis⁷ is needed.

Define the LinCov dispersion state vector to consist of trajectory position and velocity dispersions δr , δv . Augment this state with two maneuver states Δv_1 , Δv_2 , and two variable constraint time states δt_{c1} and δt_{c2} , i.e., $\delta X = [\delta r, \delta v, \Delta v_1, \Delta v_2, \delta t_{c1}, \delta t_{c2}]^T$, where $\dot{\Delta v}_1 = \dot{\Delta v}_2 = \dot{\delta t}_{c1} = \dot{\delta t}_{c2} = 0$. It is assumed that the STM for this state vector is available and denoted by $\Phi_C(t_2, t_1)$ for coasting flight, for arbitrary times t_1, t_2 .

At the nominal initial time t_0^* , the initial LinCov state dispersion vector is given by $\delta X_0 = [\delta r_0, \delta v_0, 0_{8 \times 1}]^T$, and the initial LinCov dispersion covariance is

$$P_0 = \begin{bmatrix} P_{r_0 r_0} & P_{r_0 v_0} & 0_{3 \times 8} \\ P_{v_0 r_0} & P_{v_0 v_0} & 0_{3 \times 8} \\ 0_{8 \times 3} & 0_{8 \times 3} & 0_{8 \times 8} \end{bmatrix} \quad (107)$$

This initial state dispersion and covariance is propagated forward up to the time just before the targeting algorithm is called according to

$$\delta X_{tgt}^- = \Phi_C(t_{tgt}^*, t_0^*) \delta X_0 \quad (108)$$

$$P_{tgt}^- = \Phi_C(t_{tgt}^*, t_0^*) P_0 \Phi_C(t_{tgt}^*, t_0^*)^T \quad (109)$$

When the targeting algorithm is executed at time t_{tgt}^* , the dispersion of the impulsive maneuvers Δv_1 , Δv_2 , and the dispersion of the variable constraint times δt_{c1} and δt_{c2} , are computed and given by

$$\begin{bmatrix} \Delta v_1 \\ \Delta v_2 \\ \delta t_{c1} \\ \delta t_{c2} \end{bmatrix} = \mathcal{P}_{\Delta V, \delta T} \begin{bmatrix} \delta r_0 \\ \delta v_0 \end{bmatrix} \quad (110)$$

where the partial derivative $\mathcal{P}_{\Delta V, \delta T}$ of the impulsive maneuvers and constraint times with respect to the initial trajectory dispersion is determined from either Eq. 2, $\mathcal{P}_{\Delta V, \delta T} = \mathcal{M}^{-1} \mathcal{N}$, or Eq. 3, $\mathcal{P}_{\Delta V, \delta T} = (\mathcal{M}^T W_\psi \mathcal{M})^{-1} \mathcal{M}^T W_\psi \mathcal{N}$, or Eq. 4, $\mathcal{P}_{\Delta V, \delta T} = (W_c \mathcal{M}^T (\mathcal{M} W_c \mathcal{M}^T)^{-1} \mathcal{N}$, and where the matrices \mathcal{M} and \mathcal{N} are given by Eqs. 20 and 21.

Based on Eq. 110, the effect of the targeting algorithm is to “correct” the LinCov state dispersion and covariance at time t_{tgt}^* according to

$$\delta X_{tgt}^+ = \begin{bmatrix} I_{6 \times 6} & 0_{6 \times 8} \\ \mathcal{P}_{\Delta V, \delta T} & 0_{8 \times 8} \end{bmatrix} \delta X_{tgt}^- = \Phi_{tgt} \delta X_{tgt}^- \quad (111)$$

$$P_{tgt}^+ = \Phi_{tgt} P_{tgt}^- \Phi_{tgt}^T$$

where the single subscript on Φ_{tgt} denotes an instantaneous state-correction matrix used to correct δX_{tgt} and P_{tgt} at time t_{tgt}^* .

Next, the state dispersion and covariance are propagated to the first nominal maneuver execution time $t_{\Delta v_1}^*$.

$$\delta X_{\Delta v_1}^- = \Phi_C(t_{\Delta v_1}^*, t_{tgt}^*) \delta X_{tgt}^+ \quad (112)$$

$$P_{\Delta v_1}^- = \Phi_C(t_{\Delta v_1}^*, t_{tgt}^*) P_{tgt}^+ \Phi_C(t_{\Delta v_1}^*, t_{tgt}^*)^T \quad (113)$$

At the nominal maneuver time $t_{\Delta v_1}^*$, the effect of executing Δv_1 is to again “correct” the LinCov state dispersion and covariance according to

$$\delta X_{\Delta v_1}^+ = \delta X_{\Delta v_1}^- + \mathcal{P}_{\delta v} \Delta v_1 \quad (114)$$

$$= [I + \mathcal{P}_{\delta v} \mathcal{P}_{\Delta v_1}] \delta X_{\Delta v_1}^- \quad (115)$$

$$= \Phi_{\Delta v_1} \delta X_{\Delta v_1}^- \quad (116)$$

$$P_{\Delta v_1}^+ = \Phi_{\Delta v_1} P_{\Delta v_1}^- \Phi_{\Delta v_1}^T \quad (117)$$

where $\mathcal{P}_{\delta v}$ is the partial derivative of δX with respect to δv , $\mathcal{P}_{\Delta v_1}$ is the partial derivative of Δv_1 with respect to δX , and $\Phi_{\Delta v_1} = [I + \mathcal{P}_{\delta v} \mathcal{P}_{\Delta v_1}]$ denotes an instantaneous state-correction matrix used to correct $\delta X_{\Delta v_1}$ and $P_{\Delta v_1}$ at time $t_{\Delta v_1}^*$.

Next, the LinCov state dispersion and covariance is propagated from $t_{\Delta v_1}^*$ to the first nominal constraint time $t_{c_1}^*$ using

$$\delta X_{c_1}^- = \Phi_C(t_{c_1}^*, t_{\Delta v_1}^*) \delta X_{\Delta v_1}^+ \quad (118)$$

$$P_{c_1}^- = \Phi_C(t_{c_1}^*, t_{\Delta v_1}^*) P_{\Delta v_1}^+ \Phi_C(t_{c_1}^*, t_{\Delta v_1}^*)^T \quad (119)$$

At the nominal constraint time $t_{c_1}^*$, the effect of the variable constraint time δt_{c_1} on the state dispersion is

$$\delta X_{c_1}^+ = \delta X_{c_1}^- + \dot{X}_{c_1}^* \delta t_{c_1} \quad (120)$$

$$= \left[I + \dot{X}_{c_1}^* \mathcal{P}_{\delta t_{c_1}} \right] \delta X_{c_1}^- \quad (121)$$

$$= \Phi_{c_1} \delta X_{c_1}^- \quad (122)$$

where $\mathcal{P}_{\delta t_{c_1}}$ is the partial derivative of δt_{c_1} with respect to the LinCov state dispersion vector δX , $\dot{X}_{c_1}^*$ is the nominal state time-derivative at time $t_{c_1}^*$, and $\Phi_{c_1} = \left[I + \dot{X}_{c_1}^* \mathcal{P}_{\delta t_{c_1}} \right]$ denotes an instantaneous state-correction matrix at time $t_{c_1}^*$. Using the equation above, the effect of the variable constraint time δt_{c_1} on the LinCov dispersion covariance is

$$P_{c_1}^+ = \Phi_{c_1} P_{c_1}^- \Phi_{c_1}^T \quad (123)$$

The LinCov state dispersion and covariance is then propagated to the next maneuver time $t_{\Delta v_2}^*$ using

$$\delta X_{\Delta v_2}^- = \Phi_C(t_{\Delta v_2}^*, t_{c_1}^*) \delta X_{c_1}^+ \quad (124)$$

$$P_{\Delta v_2}^- = \Phi_C(t_{\Delta v_2}^*, t_{c_1}^*) P_{c_1}^+ \Phi_C(t_{\Delta v_2}^*, t_{c_1}^*)^T \quad (125)$$

and corrected to account for the execution of Δv_2 using

$$\delta X_{\Delta v_2}^+ = \delta X_{\Delta v_2}^- + \mathcal{P}_{\delta v} \Delta v_2 \quad (126)$$

$$= [I + \mathcal{P}_{\delta v} \mathcal{P}_{\Delta v_2}] \delta X_{\Delta v_2}^- \quad (127)$$

$$= \Phi_{\Delta v_2} \delta X_{\Delta v_2}^- \quad (128)$$

$$P_{\Delta v_2}^+ = \Phi_{\Delta v_2} P_{\Delta v_2}^- \Phi_{\Delta v_2}^T \quad (129)$$

where $\Phi_{\Delta v_2} = [I + \mathcal{P}_{\delta v} \mathcal{P}_{\Delta v_2}]$ denotes an instantaneous state-correction matrix at time $t_{\Delta v_2}^*$.

Lastly, the LinCov state dispersion and covariance is propagated to the nominal time of the second constraint $t_{c_2}^*$ using

$$\delta X_{c_2}^- = \Phi_C(t_{c_2}^*, t_{\Delta v_2}) \delta X_{\Delta v_2}^+ \quad (130)$$

$$P_{c_2}^- = \Phi_C(t_{c_2}^*, t_{\Delta v_2}^*) P_{\Delta v_2}^+ \Phi_C(t_{c_2}^*, t_{\Delta v_2}^*)^T$$

and again corrected for the variable constraint time, δt_{c_2} in a manner similar to δt_{c_1} .

$$\delta X_{c_2}^+ = \delta X_{c_2}^- + \dot{X}_{c_2}^* \delta t_{c_2} \quad (131)$$

$$= \left[I + \dot{X}_{c_2}^* \mathcal{P}_{\delta t_{c_2}} \right] \delta X_{c_2}^- \quad (132)$$

$$= \Phi_{c_2} \delta X_{c_2}^- \quad (133)$$

$$P_{c_2}^+ = \Phi_{c_2} P_{c_2} \Phi_{c_2}^T \quad (134)$$

where $\Phi_{c_2} = \left[I + \dot{X}_{c_2}^* \mathcal{P}_{\delta t_{c_2}} \right]$